Scaling of Airfoil Self-Noise Using Measured Flow Parameters

Thomas F. Brooks* and Michael A. Marcolini*
NASA Langley Research Center, Hampton, Virginia

Data from an airfoil broadband self-noise study are reported. Attention here is restricted to two-dimensional models at zero angle of attack to the flow. The models include seven NACA 0012 airfoil sections and five flat plate sections with chordlengths ranging from 2.54 to 60.96 cm. Testing parameters include flow velocity to 71.3 m/s and boundary-layer turbulence through natural transition and by tripping. Detailed aerodynamic measurements are conducted in the near-wake of the sharp trailing edges. The noise spectra of the self-noise sources are determined by the use of a cross-spectral technique. The acoustic data are normalized using the measured aerodynamic parameters in order to evaluate a commonly used scaling law. An examination of the Reynolds number dependence of the normalized overall levels has revealed a useful scaling result. This result appears to quantify the transition between turbulent boundary-layer trailing-edge noise and laminar boundary-layer vortex shedding noise.

Introduction

RECENT progress in research on rotor broadband noise sources is reviewed by Brooks and Schlinker.[1] Of concern here is broadband self-noise generation for airfoil blades encountering smooth uniform flow at small angles of attack. At high Reynolds number (*Re*), turbulent boundary layers (TBL) develop over most of the airfoil. Noise is produced due to the passage of this turbulence over the trailing edge (TE). At low *Re*, largely laminar boundary layers (LBL) develop whose instabilities result in vortex shedding (VS) and its associated noise from the TE.

Recently, Brooks and Hodgson[2] demonstrated, using measured pressures, that if sufficient information is known about the TBL convecting surface pressure field then the noise can be accurately predicted. Schlinker and Amiet[3] employed a generalized empirical description of surface pressure to predict measured noise. However, the lack of agreement for some cases indicated a need for a more accurate pressure description which is not available presently. In the same study a different but established approach was used to normalize the available noise data. This simpler approach is based on the Ffowcs Williams and Hall[4] edge-scatter formulation. A scaling law prediction equation was fitted to the data using only a mean TBL parameter, thickness δ. Where the TBL thickness was unknown, simple flat plate theory was used to estimate δ. Spectral data initially differing by 40 dB coalesced within 7 dB, consistent with the results of the other approach. The extent to which data scatter was caused by the uncertainty in the actual value of δ was unknown.

The other self-noise source considered here is due to vortex shedding, which occurs when a LBL exists over most of at least one side of the airfoil. The LBL-vortex shedding is apparently coupled to acoustically excited aerodynamic feedback loops.[5-7] In Refs. 6 and 7 the feedback loop is taken to be between the airfoil TE and an upstream "source" point on the surface. The resulting noise spectrum is composed of a number of quasitones related to the shedding rates at the TE. The gross trend of the frequency dependence was found by Paterson et al.[8] to scale on a Strouhal number basis with the LBL thickness at the TE being the relevant length scale. In a more sophisticated development, Fink[7] later related the frequency dependence to LBL instability theory. In both cases[7,8] a simple flat plate LBL theory was used to determine the BL thickness parameters. It is noted that no method has been developed to predict absolute sound levels for this source.

An airfoil self-noise study is being conducted at NASA Langley Research Center to provide a comprehensive data base for the evaluation and development of prediction methods. The data should provide a basis for fashioning a rotor broadband noise prediction program. Tested are isolated nonrotating models. The models include a comprehensive array of two- and three-dimensional airfoil and flat plate sections. All models have very sharp trailing edges. Detailed aerodynamic and acoustic data are obtained for a large number of parametric combinations.

Data are presented herein for the two-dimensional zero angle-of-attack cases. For the first time the quantitative relationship between TBL-TE and LBL-VS noise sources, as well as the *Re*-dependent transitional behavior between the sources, are examined. Importantly, the acoustic data are normalized using measured TE flow data rather than approximations for each test condition to allow assessment of current broadband noise scaling-law prediction capabilities. Particular attention is given to *Re* effects not addressed previously.

Description of Experiment

The models were tested in the low-turbulence potential core of a free jet in the anechoic quiet-flow facility at the research center. The free jet was provided by a vertically mounted nozzle with rectangular exit dimensions of 0.3×0.46 m. The turbulent intensity was less than 0.05% at the center of the nozzle exit. Additional details of the facility, testing hardware, and instrumentation are given in Refs. 2 and 9.

Test Models

Most of the aluminum models used for the tests are shown in Fig. 1. At the top left of this figure is one of the three-dimensional test airfoils whose data are not reported here. Shown for the two-dimensional models, all of 45.72 cm span, are the 2.54, 5.08, 10.16, 15.24, 22.86, 30.48, and 60.96 cm chord NACA 0012 airfoils and also the 10.16, 15.24, 22.86, and 30.48 cm chord flat plate models. Not shown is the 60.96 cm chord flat plate model. The TE of the models were made very sharp, less than 0.05 mm thick, without beveling the edge. The flat plate's maximum leading edge (LE) thickness is 0.1 mm. For the airfoils the slope of the surface near the uncusped TE corresponds to 7 deg off the chordline. For the flat

Received June 28, 1983; revision received March 12, 1984. This paper is declared a work of the U.S. Government and therefore is in the public domain.

*Aerospace Technologist, Aeroacoustics Branch, Acoustics and Noise Reduction Division.

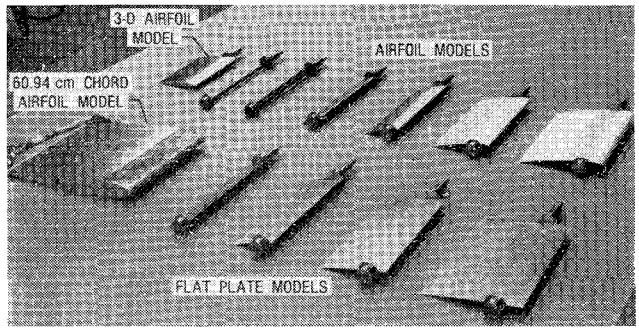

Fig. 1 Test airfoil and flat plate models.

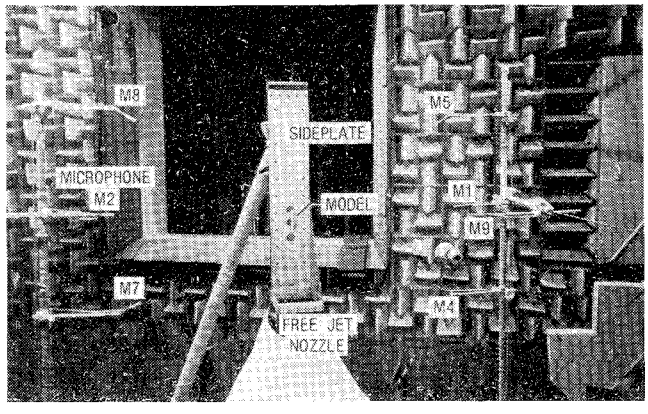

Fig. 2 Test setup for noise measurement with a 3-D model case shown for clarity.

plates (maximum thickness of 3% of chordlength C) the corresponding slope is 1.7 deg off the chordline.

At the spanwise extremes of the models are attached cylindrical hubs that provide support and flush mounting to the sideplates of the test rig. For all models at the geometric angle of attack of $\alpha_g = 0$ deg, the TE is located 61.0 cm above the nozzle exit. In Fig. 2 an acoustic test configuration in the chamber is shown. A three-dimensional case is shown so that the model can be seen fitted to the sideplate. The sideplates ($152.4 \times 30.0 \times 1$ cm) are heavily reinforced and flush mounted to the nozzle lips. For the two-dimensional cases, which are the subject of this paper, an additional sideplate is used.

Instrumentation

For the acoustic tests eight 0.5 in. (1.27 cm) free-field-response microphones were fixed mounted in the plane perpendicular to the two-dimensional model midspan. One microphone was offset from this. Figure 2 shows seven of these with the identification numbers indicated. Microphones M1 and M2 are perpendicular to the chordline at the TE for $\alpha_g = 0$ deg. The other microphones shown are at radii of 121.9 cm from the TE, as with M1 and M2, but are positioned 30 deg forward and 30 deg aft. The calibrations, signal conditioning, and recording techniques used for the acoustic data acquisition are the same as for Ref. 2, where details are given. The data reduction is also the same, except here the computer-interfaced signal processor employed an average of 1024 samples rather than 256. With the data analyzed to a frequency of 20 kHz the analysis bandwidth is 40 Hz.

For the aerodynamic tests the microphones to the right in Fig. 2 were removed and replaced by a large three-axis computer-controlled traverse rig used to position hot-wire probes. The probes included both cross-wire and single-wire configurations. The probes were used to survey the flowfields about the models, especially in the boundary-layer/near-wake region just downstream of the trailing edge. For the single-wire probe the 1.2 mm length wire was aligned with the trailing edge. The miniature cross-wire probes had a distance between the wire prongs of 0.5 mm. Each of the wire channels consisted of a constant-temperature anemometer, linearizer, and filter.

Test Conditions

For the two-dimensional airfoil cases reported, freestream velocities U_0 between 23.8 and 71.3 m/s were tested corresponding to a Mach number range from 0.069 to 0.208 and an Re range, based on chord, from 4.8×10^4 to 2.5×10^6. Factors promoting true two-dimensional flow behavior about the models include large aspect ratio (smaller models), boundary-layer tripping, and small adverse pressure gradients (small α_g and flat plate cases). Data are given here for $\alpha_g = 0$ deg. Results for the large 60.96 cm chord airfoil are given only for the tripped cases where two-dimensional flow was verified.[2]

For the untripped model cases (natural BL development) the surfaces were smooth and clean. For the tripped cases the BL transition was achieved by a random distribution of grit in strips from the LE to 20% chord. This tripping is considered "heavy" because of the chordwise extent of the strip and is not optimum from purely aerodynamic considerations. Its use was based on the desire to establish a well-developed TBL even for the smaller models and at the same time retain geometric similarity. The commercial grit number[10] was 60, with a density of about 380 particles/cm^2. An exception was the 2.54 chord airfoil which had a 30% chord strip with number 100 grit at about 690 particles/cm^2. Also, since acoustic data for the 60.96 cm chord airfoil from Ref. 2 were used, 2-cm-wide strips of number 40 grit at 15% chord were used here for the aerodynamic measurements.

Trailing-Edge Flow Measurements

The results presented are hot-wire probe measurements made in the boundary-layer/near-wake region of the trailing edge of the models. The probes were traversed perpendicular to the models' chordlines at various distances downstream of the trailing edges. The measurements shown here were made at 0.64 mm from the trailing edge of the 2.54 cm chord airfoil and at 1.3 mm for the other models. The integral parameters —displacement thickness δ^* and momentum thickness θ—are calculated from the measured single-wire mean velocity profiles. The calculations require the knowledge of the TE boundary-layer thickness δ, where the mean velocity reaches 99% of the potential flow stream velocity. The potential flowfield is curved near the model thereby complicating the choice of δ. The values of δ were chosen based on detailed examinations of the respective turbulent-velocity and Reynolds-stress distributions from the cross-wire measurements as well as the mean profiles. The estimated accuracy[9] of δ is within $\pm 5\%$ for TBL flow and $\pm 10\%$ for laminar and transitional cases. These correspond respectively to calculated variances of $\pm 1.5\%$ and $\pm 3\%$ for both δ^* and θ.

The TE boundary-layer parameters δ, θ, and H $(= \delta^*/\theta)$ for the airfoil and flat plate models of different sizes for a range of test conditions are given in Fig. 3. To aid comparison, simple flat plate theoretical values at the TE are shown for reference. Interestingly for the untripped airfoil cases in Fig. 3a the 1/7th power law, calculated assuming that the BL is fully turbulent at the LE, is in fair quantitative agreement. When the BL's are tripped the thicknesses increase, dependence on velocity decreases, and the trend with chord-length stabilizes. In Fig. 3b for flat plates the transitional behavior for the untripped cases is well demonstrated. As the velocity increases the LBL characteristics, generally agreeing here with the Blasius solution, give way to trend characteristics of TBL flows. Tripping results in thicker well-developed TBL flows.

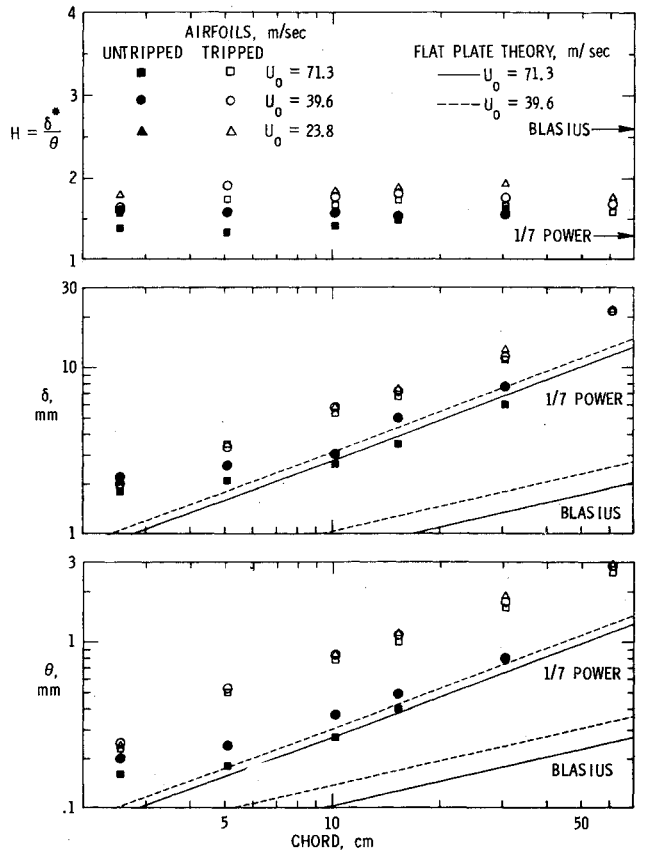

a) Airfoils.

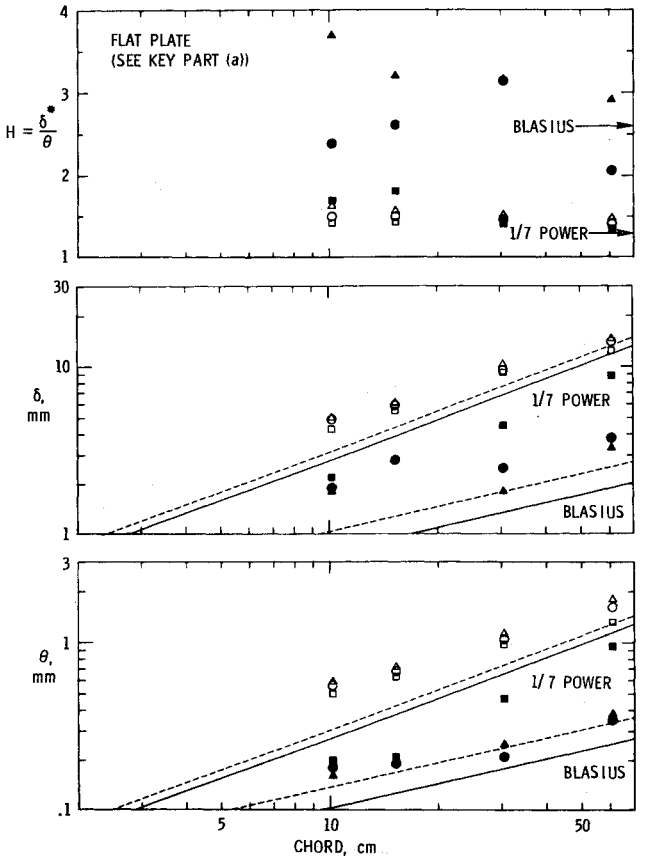

b) Flat plates.

Fig. 3 Trailing-edge near-wake thicknesses of models as a function of chordlength and BL tripping for several velocities.

Acoustic Measurements

Source Localization

In Fig. 4 the upper curves are the cross-correlations, $R_{12}(\tau) = \langle p_1(t)p_2(t+\tau)\rangle$, between the sound pressure signals p_1 and p_2 of microphones M1 and M2, identified in Fig. 2, respectively. The cases are for the tripped 30.48 cm chord airfoil mounted in the test rig and also where the airfoil is removed. Because the microphones are on the opposite sides of and at equal distance from the airfoil, one expects and sees a negative correlation peak at the signal delay time $\tau = 0$. This correlation is indicative of a broadband noise source of dipole character, whose phase is reversed on opposing sides. When the airfoil is removed the strong negative peak disappears, leaving the contribution from the test rig alone. The most coherent parts of this noise are from the lips of the nozzle which are, as with the airfoil noise, of a dipole character. The microphone time delays predicted for these sources are indicated by arrows. The predictions[11,2] account for the effect of the refraction of sound by the free jet shear layer as well as the pure geometric relationship, between the microphones and the hardware, and the speed of sound.

Much is revealed about the self-noise sources from the cross-correlations, $R_{45}(\tau)$, between M4 and M5 shown as the lower curves of Fig. 4. The predicted delay times again appear to correctly identify the correlation peaks associated with the noise emission locations. The peaks are positive for $R_{45}(\tau)$ because both microphones are on the same side of the dipole's directional lobes. The noise field is seen to be dominated by trailing edge noise. Any contribution to the noise field from the LE would appear where indicated in the figure. As is subsequently shown, there are contributions in many cases. For such cases it is seen that the negative correlation peak for $R_{12}(\tau)$ would be the sum of the TE and LE correlation peaks brought together at $\tau = 0$ and inverted in sign.

The correlations $R_{45}(\tau)$ are shown in Fig. 5 for the airfoils and in Fig. 6 for the flat plates for different chord sizes. In both cases the BL's are tripped. The TE noise correlation peaks are at $\tau = -0.11$ ms for all cases because at $\alpha_g = 0$ deg the TE location of all models are the same. The LE location changes with chord size.

For the larger airfoil cases of Fig. 5 the TE contribution is seen to dominate the noise field. As the chord decreases the LE noise peaks increase to become readily identifiable in the correlation. At the smallest chord the LE contribution is even somewhat more than that of the TE. It is noted that there appears to be an extraneous source of discrete low-frequency noise contributing to the 22.86 cm chord correlation.

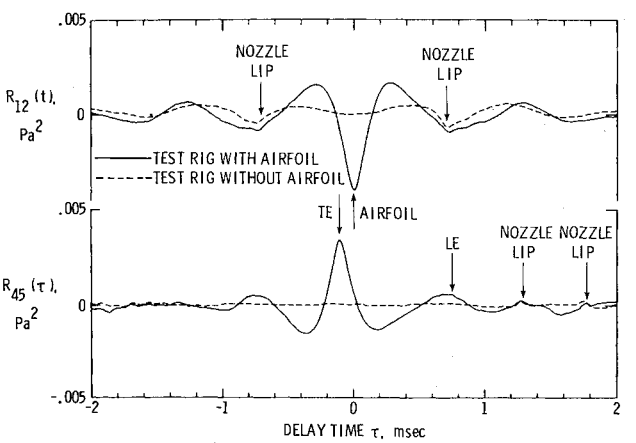

Fig. 4 Cross-correlations between microphones M1 and M2, and between M4 and M5, for the tripped 30.48 chord airfoil mounted at $\alpha_g = 0$ deg in the test rig, $U_0 = 71.3$ m/s. Arrows indicate predicted values of τ for different source positions.

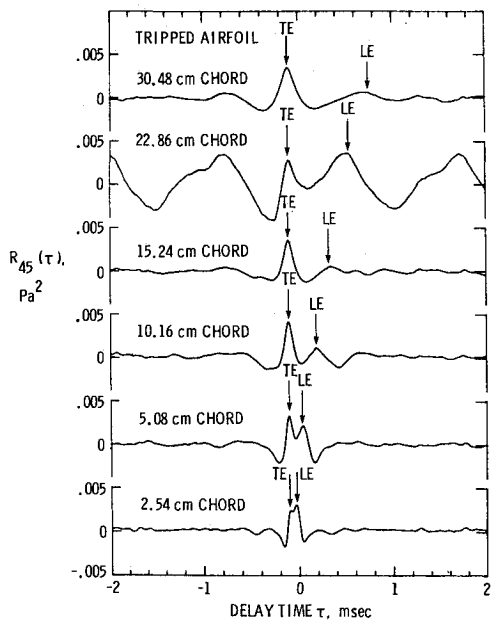

Fig. 5 Cross-correlations between M4 and M5 for tripped airfoil cases of different chord sizes, $U_0 = 71.3$ m/s. Arrows indicate predicted values of τ.

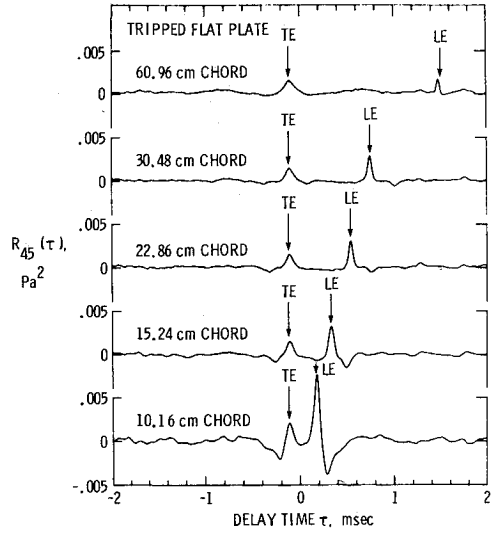

Fig. 6 Cross-correlations between M4 and M5 for tripped flat plate cases of different chord sizes, $U_0 = 71.3$ m/s. Arrows indicate predicted values of τ.

For the flat plate cases of Fig. 6 the situation is different from that of the airfoils. Here the LE contribution to the correlation is always more than that of the TE, more so for the smaller chords. It should be noted that precise interpretation of the peak correlation amplitude for the LE is subject to directivity and shear layer correction considerations associated with the changing position of the LE. These effects are not accounted for here.

The character of the TE noise as reflected in the correlations is as expected. However, an initial review of the contributions from the LE can lead to interesting speculation about its origin. Suspect may be the grit about the LE used for BL tripping. However, correlations for the untripped cases (not given here) also show the presence of this LE source, indicating the grit does not significantly contribute to the noise.

Another speculative origin of LE noise would be that the upstream near-field of the TE noise is diffracted around the LE and radiated to the microphones. This would be an acoustic-compactness effect not accounted for in TE theory. Also, this would have great implication as to how the present noise data are interpreted and utilized. However this hypothesis can be discredited for several reasons. First, one would expect with this hypothesis that the LE contribution should increase, but remain less than the TE contribution, with decreasing chordlength for both the airfoil and the flat plate cases. This is decidedly not the case for the flat plate data. Even within the context of the airfoil correlations alone, contradictions are found as follows. If the LE source is as hypothesized, by necessity it would be strongly coherent with the TE source but delayed in emission time by that required to propagate upstream to the LE. A simple calculation on what the cross-correlation $R_{45}(\tau)$ should look like for this case shows that four peaks, not two, should occur in the correlation. The result for $R_{45}(\tau)$ for the 2.54 cm chord airfoil case of Fig. 5 can be used for comparison. In addition to that predicted for the TE and LE, at $\tau = -0.11$ and -0.036 ms, respectively, strong negative peaks would be predicted at $\tau = 0.019$ and 0.166 ms. The lack of such peaks demonstrates that the LE and TE sources are uncorrelated.

The actual origin of LE noise appears to be inflow turbulence to the LE from the TBL of the test rig's side plates. This should be the case even though the spanwise extent of this TBL is small compared to the portion of the models that encounter uniform low-turbulence flow from the nozzle. Inflow turbulence can be a very efficient noise mechanism.[12] Its full efficiency can be obtained however only when the model's LE is very sharp. Such is the case for the flat plates where the LE noise maintains its high levels for all chord sizes. The reason the LE noise contributions diminish for the larger chords of the airfoil cases can be attributed to the proportional increase in LE radius with chord. When this thickness increases to a size that is large in comparison to the turbulent scale in the sideplate TBL, then the sectional lift fluctuations associated with inflow turbulence noise are not developed.

Spectral Characteristics

The cross spectrum between microphones M1 and M2, say $G_{12}(f)$, is the Fourier transform of $R_{12}(\tau)$. If the contributions from the LE, nozzle lips, and any other coherent extraneous-source locations were removed, then $G_{12}(f)$ would equal the autospectrum of the airfoil TE self-noise, $S(f)$. Actually, the relationship would be $G_{12}(f) = S(f)\exp i(2\pi f\tau \pm \pi)$, where τ is the delay time of the TE correlation peak. This approach is formalized elsewhere.[2]

The spectra for this report were found from $G_{12}(f)$, determined with the models in the test rig, after a point-by-point vectorial subtraction of $G_{12}(f)$, determined with the airfoil removed. This is equivalent to subtracting corresponding $R_{12}(\tau)$ results of Fig. 4 and then taking the Fourier transform. This procedure results in "corrected" spectra which are devoid of at least a portion of the background test-rig noise, primarily emitted from the nozzle lips. The backgrounds were not subtracted for the 60.96 cm chord cases where the large surface blocks and reflects test rig noise making subtraction of the spectra inappropriate.

These "corrected" data still contain contamination from the inflow-turbulence LE noise contribution. A practical method to cleanly extract TE noise is believed to entail the direct Fourier transform of $R_{45}(\tau)$ data which have been edited to eliminate the LE contribution. This has not been accomplished for the spectral and overall sound pressure level (OASPL) data of this paper. For this reason, flat plate model acoustic data are reported only to the extent LE noise contamination could be eliminated. Airfoil cases are given with a cautionary note for the smaller chords where the contamination is highest. Judging from the relative levels of the correlation peaks of $R_{45}(\tau)$ for the tripped cases in Fig. 5, the OASPL, determinable from $G_{12}(f)$, should overestimate the TE noise for the 2.54, 5.08, 10.16, and 15.24 cm chord cases by

approximately 3.5, 2.0, 1.0, and 0.6 dB, respectively. How the details of the spectrum are affected is not known. For the untripped cases, where vortex shedding noise is evident, the levels as presented are accurate.

Self-noise spectra results are given for a large and a small airfoil in Fig. 7 for the tripped and untripped cases. The measured spectra are cut at the low and high frequencies where corresponding phase indicates the noise is from sources other than that of the airfoil. The apparent spectral interference pattern seen at the lowest levels for the higher frequencies is a remnant of the background noise subtraction process.

For the large airfoil it is seen in Fig. 7 that the effect of tripping the BL near the LE is to increase the lower frequency noise and produce a more rapid dropoff in level for the higher frequencies. The spectral levels for the smaller tripped airfoil are compatible with those of the much larger airfoil. However, when the BL tripping is removed, a rather imposing contribution to the noise field results. The vortex shedding noise seen centered near 10 kHz is composed of a number of discrete tones.

Scaling Approach

A primary purpose of this paper is to normalize trailing edge self-noise data to assess current scaling law capability. The fundamental scaling law is based on the analysis of Ffowcs Williams and Hall.[4] For the problem of turbulence convecting at low subsonic velocity U_c above a large rigid plate and past the TE into the wake, the result is

$$\langle p^2 \rangle \sim \rho_0^2 v'^2 \frac{U_c^3}{a_0}\left(\frac{Ll}{R^2}\right)\bar{D} \qquad (1)$$

where $\langle p^2 \rangle$ is the overall mean-square sound pressure at the observer location at R, ρ_0 the medium density, v'^2 the mean-square turbulence velocity, a_0 the speed of sound, l a characteristic turbulence correlation scale, and L the spanwise extent of the edge wetted by the flow. The directivity factor $\bar{D}$ equals 1 for observers normal to the surface from the TE. The usual assumptions are that $v' \sim U_c$, $U_c \sim U_0$, and $l \sim \delta$(or δ^*). Fink[13] assumes a universal spectrum shape $F_1(St)$ for the noise, where St is the Strouhal number $f\delta/U_0$. $F(St)$ depends functionally only on the ratio of St to its peak value, St_{peak}. The empirical function is based on "clean" airframe noise data where TBL-TE was assumed to be the most dominant source. From this the following normalization form is found for the one-third octave sound pressure level.

$$\mathrm{SPL}_{\frac{1}{3}} - 10\log\left[\left(\frac{U_0}{100}\right)^5 \frac{\delta L}{R^2}\right] = F_1(St) + K_1 \qquad (2)$$

with $\mathrm{SPL}_{\frac{1}{3}} = \mathrm{OASPL} + F_1(St)$ and K_1 is an empirical constant found when the velocity U_0 is in knots.

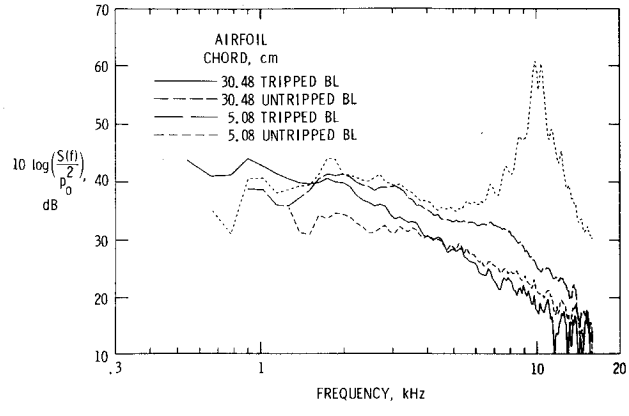

Fig. 7 Self-noise spectrum for a large and a small airfoil showing the effect of boundary-layer tripping, $U_0 = 71.3$ m/s. Levels are referenced to 1 Hz bandwidth and $p_0 = 20$ μPa.

In the scaling of the acoustic data to follow, normalizations using the measured thicknesses δ are shown. The integral parameters δ^* and θ were also used for some cases but are not shown because the results were very similar.

Spectral Results

Trailing edge self-noise for the tripped airfoils of different chord sizes are shown normalized in Fig. 8, as based on Eq. (2). The data are seen to coalesce fairly well for the higher values of St. The aforementioned LE noise contamination should be inconsequential for airfoils of 15.24 cm chords and larger. However, the effects on the spectra for the smaller airfoils could partially but not totally account for the lack of coalescence of data at the lower Strouhal numbers. Also shown in Fig. 8 is the suggested scaling law curve from Ref. 3. For the present data, if one would ignore for sake of example the low St results for the smaller chords, a better curve fit would have a more rapid falloff for increasing frequency and a change in St_{peak} from 0.1 to about 0.25 or 0.3.

Normalized spectra for various freestream velocities are shown in Fig. 9 for a large and a small airfoil, again with tripped BL's. For the individual airfoils the spectra indicate that St_{peak} increases for decreasing velocity but normalized peak levels appear about constant. The smaller airfoil has reduced St_{peak} values and increased normalized levels that cannot be attributed to the extraneous noise contamination, whose total effect should be only about 1.0 dB.

The normalized results for the untripped airfoils of different chord sizes are shown in Fig. 10. For the larger airfoils, well-developed TBL's are present over most of the chord, resulting in spectra similar to those for the tripped BL cases. However, for the smaller airfoils, the low Reynolds numbers lead to largely laminar BL's whose instabilities result in vortex shedding. As expected the spectra are seen not to coalesce, but as in Ref. 8, the dominant frequencies for the vortex shedding noise are seen generally to scale on a Strouhal basis with BL thickness.

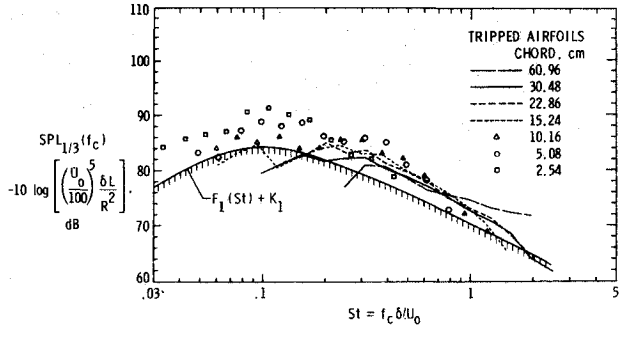

Fig. 8 Normalized one-third octave spectra. Effect of chord size for airfoils with tripped boundary layers, $U_0 = 71.3$ m/s.

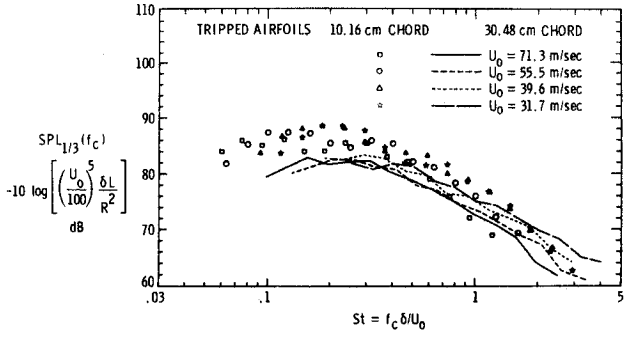

Fig. 9 Normalized spectra. Effect of freestream velocity for a large and a small tripped airfoil.

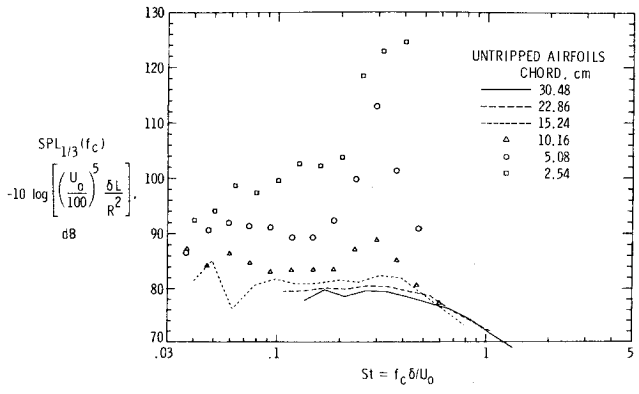

Fig. 10 Normalized spectra. Effect of chord size for airfoils with untripped boundary layer, $U_0 = 71.3$ m/s.

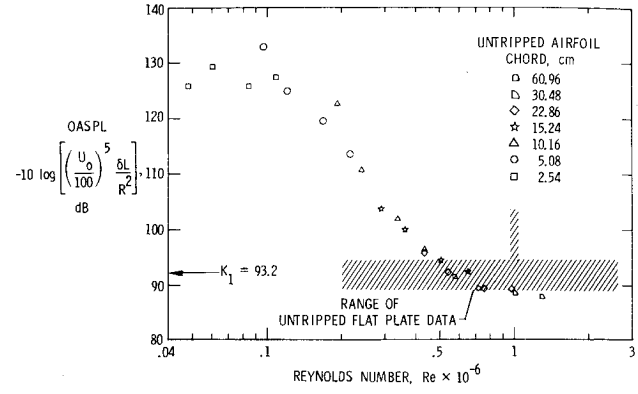

Fig. 12 Effects of Reynolds number on normalized overall sound pressure levels for the untripped airfoil cases. Region of flat plate results is shown.

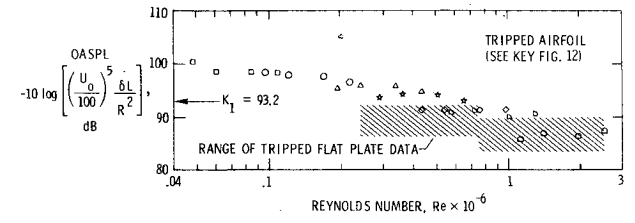

Fig. 11 Effects of Reynolds number on normalized overall sound pressure levels for the tripped airfoil cases. Region of flat plate results is shown.

Reynolds Number Results

The overall self-noise levels for the tripped airfoils of the various chord sizes and velocities are shown normalized in Fig. 11 in terms of the Reynolds number based on the chord. The results show that for a given airfoil the levels collapse quite well to a constant level. The level suggested by Ref. 3, shown as K_1, appears appropriate at least for the midrange of the airfoil sizes. In general, the normalized levels decrease for increasing chord. If the aforementioned noise contamination was removed, the amplitude of the data at the lower values of *Re* would be reduced somewhat but the trend shown would remain.

Also shown in Fig. 11 is a shaded region indicating where tripped flat plate self-noise data would be after the elimination of LE noise contamination. The normalized levels are compatible to the airfoils for higher *Re* values.

In Fig. 12 are shown the normalized overall self-noise levels, again in terms of *Re*, where the boundary-layer transition to turbulence was allowed to develop naturally. For these airfoil results, since vortex shedding noise dominates the lower *Re* ranges, the effect of LE noise contamination is negligible. The "reversed-S" shaped coalescence curve shown appears to quantify the levels of and transition between TBL-TE noise and LBL-VS noise. This should prove to be a significant result. There is some indication in data not shown that the curve should remain similar but shift to the right for increasing angles of attack.

Another key result shown in Fig. 12 is that, unlike for the airfoil models, vortex shedding did not generally occur for the flat plate models in spite of the seemingly well-suited laminar and transitory BL conditions that existed. Previous LBL-VS experimental studies considered only airfoil shapes. The present result is important as it points to a necessary refinement of existing theory for vortex shedding. Vortex shedding requires the establishment of a so-called aerodynamic "source" point on the surface where laminar instability waves originate and convect downstream to the TE to produce noise. The acoustic waves propagate upstream to complete feedback loops by reinforcing or weakening the disturbances at the source point. It is suggested that the absence of vortex shedding for flat plates is due to the lack of a chordwise pressure gradient variation. This pressure gradient effect helps to establish and fix the location of a "source" point for practical airfoil shapes. The potential importance of this effect was mentioned but not incorporated in an analysis of Ref. 7.

Discussion of Results

Near-wake flow measurements are reported for an array of two-dimensional, sharp-edge models. Trailing-edge "boundary-layer" thickness parameters, needed to normalize corresponding acoustic data, were determined for both naturally developed and artificially transitioned boundary layers.

Acoustic data are presented for both the low and high *Re* self-noise mechanisms. These are, respectively, LBL-vortex shedding noise and TBL-trailing edge noise. Spectra and overall levels are normalized using measured BL thicknesses rather than simple approximations. This allows a quantitative assessment of current scaling law capabilities. The results are dependent on whether the BL's were tripped or untripped.

Tripping is a means to simulate high *Re* TBL conditions. It does eliminate LBL-VS noise, leaving TBL-TE noise, for all chord sizes and velocities tested. For spectral normalization the degree of coalescence of the data is consistent with less comprehensive results from previous studies.[2,3] The spectra for the midrange of chord sizes tested (15.24–30.48 cm) coalesce better, to well within a band range of about 5 dB. The spectral peak Strouhal numbers, based on δ, are about 0.25 or 0.3, but they are found to be somewhat dependent on both chord size and velocity. When overall levels are normalized vs *Re* based on the chord, one sees the scaling of TBL-TE noise is not independent of *Re* as has been generally assumed in the past. The levels are found to decrease somewhat with increasing *Re*. However, the data do not approach a single curve, which shows that scaling is not uniquely dependent on *Re*. This indicates that other factors, such as the method of BL tripping, may affect the accuracy of scaling.

As expected, for the airfoil cases with untripped BL's, the spectral normalizations appeared to coalesce data only for the larger airfoils with well-developed TBL's. For the smaller airfoils, the distributions of vortex shedding tones in the spectra did tend to scale in frequency on a Strouhal basis in general consistency with previous studies. When overall levels are normalized, an "inverted-S" curve results which appears to quantify the transition from LBL-VS self-noise to TBL-TE self-noise as a unique function of *Re*. This is apparently the first indication that such effects can be quantified. A detailed examination of this scaling property should be of interest in future work. However, the result can be useful now to estimate the overall levels, and at the same time determine the relative

contribution of the two self-noise mechanisms for particular lightly loaded rotor systems.

Another importance of the "inverted-S" curve result is the warning it gives that interpretation of untripped scale model rotor results, with regard to self-noise generation, can be exceedingly difficult because of the very strong influence of *Re*. Any attempts to match full-scale *Re* with small-scale rotors would likely result in domination by sources unrelated to broadband self-noise. Caution is also indicated even for scale model rotors that employ BL tripping. The present data indicate a change in normalization constants with model scale which would lead to bias errors in scaling the results. Also, in scaling one must remember that full-scale rotors that are untripped will have portions of the blades, such as inboard near the hub, undergoing vortex shedding. This effect would not be simulated by scale model rotors with BL tripping. It should be noted that many of the concerns given here for rotors should also apply to model testing of airframe noise components.

References

[1]Brooks, T.F. and Schlinker, R.H., "Progress in Rotor Broadband Noise Research," *Vertica*, Vol. 7, No. 4, 1983, pp. 287-307.

[2]Brooks, T.F. and Hodgson, T.H., "Trailing Edge Noise Prediction Using Measured Surface Pressures," *Journal of Sound and Vibration*, Vol. 78, No. 1, 1981, pp. 69-117.

[3]Schlinker, R.H. and Amiet, R.K., "Helicopter Rotor Trailing Edge Noise," AIAA Paper 81-2001, 1981; see also NASA CR-3470, Nov. 1981.

[4]Ffowcs Williams, J.E. and Hall, L.H., "Aerodynamic Sound Generation by Turbulent Flow in the Vicinity of a Scattering Half-plane," *Journal of Fluid Mechanics*, Vol. 40, March 1970, pp. 657-670.

[5]Tam, C.K.W., "Discrete Tones of Isolated Airfoils," *Journal of Acoustical Society of America*, Vol. 55, June 1974, pp. 1173-1177.

[6]Wright, S.E., "The Acoustic Spectrum of Axial Flow Machines," *Journal of Sound and Vibration*, Vol. 45, No. 2, March 1976, pp. 165-223.

[7]Fink, M.R., "Fine Structure of Airfoil Tone Frequency," United Technologies Research Center, East Hartford, Conn., Rept. 78-10, 1978.

[8]Paterson, R.W., Vogt, P.G., Fink, M.R., and Munch, C.L., "Vortex Noise of Isolated Airfoils," *Journal of Aircraft*, Vol. 10, May 1973, pp. 296-302.

[9]Brooks, T.F. and Marcolini, M.A., "Airfoil Self Noise-Effect of Scale," AIAA Paper 83-0785, April 1983.

[10]Pope, A. and Harper, J.J., *Low-Speed Wind Tunnel Testing*, John Wiley and Sons, Inc., New York, 1966.

[11]Schlinker, R.H. and Amiet, R.K., "Refraction of Sound by a Shear Layer-Experimental Assessment," AIAA Paper 79-0628, March 1979.

[12]Paterson, R.W. and Amiet, R.K., "Acoustic Radiation and Surface Pressure Characteristics of an Airfoil Due to Incident Turbulence," NASA CR-2733, Sept. 1976; also, AIAA Paper 76-571, July 1976.

[13]Fink, M.R., "Noise Component Method for Airframe Noise," AIAA Paper 77-1271, 1977.